EAI Endorsed Transactions
on Energy Web
Research Article EAI.EU

A Level-Shift Carrier PWM Modulation Technique and Predictive Current Control of a Multilevel DC-AC Converter for Interfacing Renewable Energy Sources

Vitor Pinto[1], Joao L. Afonso[1],Vitor Monteiro[1*]

[1] Centro ALGORITMI / LASI, University of Minho, 4800-058 Guimaraes, Portugal

Abstract

The integration of renewable energy sources into the electrical power grid is a crucial aspect for achieving sustainable development and reducing environmental impacts. This paper explores the implementation of a three phase Neutral Point Clamped (NPC) DC AC converter with level shift carrier PWM modulation technique and predictive current control to facilitate the grid interconnection of renewable energy systems. Multilevel converters offer important advantages over traditional two level converters, such as reduced harmonic distortion and improved efficiency. Computational simulations using the PSIM software were conducted to validate the operation of the converter, both as active rectifier and as inverter. The results demonstrated the ability of the converter to adjust its current generation, even when considering sudden power variations in the load, as well as variations in the electrical power grid. Moreover, it effectively controls the DC link voltage, while maintaining a minimal ripple in the controlled AC current. The obtained results allow to verify the robustness and reliability of the converter for the integration of renewable energy (solar photovoltaic panels) into the power grid, contributing to the pursuit of sustainable energy solutions for a greener future.

Keywords: Power Electronics, Multilevel Converter, Renewable Energy, NPC Converter, Digital Control, Predictive Control

Received on 26 October 2023, accepted on 18 July 2025, published on 28 July 2025

doi: 10.4108/ew.9802

*Corresponding author. Email: vmonteiro@dei.uminho.pt

1. Introduction

Humans have interacted with electromagnetic waves since the 6th century BC, but it wasn't until the 19th century that electricity production became feasible with the invention of Alessandro Volta's battery [1]. In the late 19th century, significant milestones such as Thomas Edison's incandescent light bulb, Nicola Tesla's alternating current (AC) generator in the first hydroelectric power plant, and Michael Faraday's transformer enabled the production and long-distance transmission of electricity [2]. This marked the beginning of an exponential improvement in human quality of life, accompanied by an ever-increasing dependency on electricity over the years.

Electricity has profoundly impacted all aspects of society, becoming essential for the vast expansion of human knowledge and indispensable for everyday life. Consequently, humans have sought to develop new methods of electricity generation. Initially, electricity was predominantly produced from fossil fuels, but their extraction led to various negative impacts, including rising sea levels and air pollution in some regions of the world. In pursuit of sustainable development, renewable energies have gained increasing attention [3].

In recent years, concerns about climate change have driven the establishment of CO2 emission reduction targets, resulting in the emergence of new energy sources on the electrical grid. These sources have introduced the concept of distributed or decentralized energy production, offering numerous benefits, including economic advantages and improved energy quality compared to traditional energy systems [4]. The proliferation of distributed electricity production has allowed new electricity providers to enter the market, fostering increased competitiveness in an industry previously dominated by major economic conglomerates.

Renewable energy sources such as wind, water, and solar power present a promising alternative to non-renewable sources as they harness natural resources that do not deplete. Additionally, renewable energy has a low environmental impact, making it a valuable choice for sustainable development. Thus, supporting and promoting the use of renewable energy sources is imperative [5].

According to Eurostat data, electricity consumption from renewable sources in Europe has been steadily increasing in recent years. In 2021, renewable energy accounted for 22% of the total gross electricity consumption in the European Union (EU) [6]. This transition towards renewable energy in electricity generation has been facilitated by the implementation of supportive policies and targets at both the European Union (EU) and national levels, alongside the continuous reduction in costs associated with renewable technologies. Wind, solar, and hydropower are the main sources of renewable electricity in the EU. Wind energy led the way in 2021, followed by solar and hydropower. However, the share of renewable energy in electricity consumption varies significantly among EU member states, with some countries relying more on renewables than others. Overall, it is expected that the use of renewable energy in electricity production will continue to grow in the coming years as more countries adopt renewable energy targets and technologies become more widespread and cost-effective.

With the focus on supplying and consuming electricity through renewable energy sources, the need arises for robust and reliable power electronics systems for power grid interconnection. In such scope, power electronics converters, are indispensable. For high power applications, multilevel converters offer a set of pertinent advantages since permits the production of a voltage waveform at their output, which is formed by combining several DC voltage sources through controlled semiconductor switching, commonly known as stepped voltage [7]. This controlled switching adds the voltages at the terminals of each capacitor on the DC-link, allowing the converter to achieve a higher output voltage while keeping the voltage across the power semiconductors lower and related to the voltages of the connected DC-link capacitors [8].

For medium (in the kW range) or high-power (in the MW range) applications, the use of multilevel converters becomes advantageous due to the limited voltage range of power semiconductors [9]. With this type of converter, semiconductors are only exposed to a voltage of Vdc/(n-1), where n is the number of levels in the converter. Apart from this advantage, stepped voltage output reduces harmonic distortion of current and voltage compared to two-level converters [9][10]. Additionally, it ensures a lower dv/dt in power semiconductors, enabling switching at lower frequencies, reducing switching losses and electromagnetic noise [9]. However, as the number of generated levels increases, the number of power semiconductors used also increases, making control more complex and implementation costly [7].

In this context, the main contributions of this paper can be highlighted as significant advancements in power electronics control and topologies for renewable energy integration: (i) it introduces a novel multilevel converter topology that achieves higher output voltage levels while minimizing voltage stresses on power semiconductors, resulting in reduced harmonic distortion and improved efficiency; (ii) the paper presents a predictive current control technique, enabling precise regulation of output current and efficient power flow control; (iii) moreover, it addresses the impact of natural DC-link voltage oscillations by implementing a sliding window average, enhancing voltage regulation stability; (iv) computational simulations using PSIM software validate the converter's successful operation as an active rectifier and inverter under various conditions, including steady and transient state. Overall, this research enhances the state-of-the-art in power electronics systems for renewable energy integration, contributing to sustainable grid development and efficient utilization of renewable resources.

The paper is organized according to the following structure. It begins with an introduction, covering the historical context of electricity production and the growing importance of renewable energy sources, particularly in Europe. The second section describes the operation principle of the multilevel converter topology and its various operating states. Following that, the control algorithm is discussed, focusing on the modulation technique, predictive current control, and the DC-link voltage control technique, and its significance in maintaining stable performance. Next, the computational validation of the proposed converter system is presented, showcasing its effectiveness in grid-side current control and DC-link voltage control. Finally, the conclusions summarize the key findings and emphasize the potential of renewable energy technologies for a sustainable future.

2. Operation Principle of the Power Converter

The presented topology is implemented using fully controlled power semiconductors and diodes. Depending on the number of semiconductors used, the number of possible levels also varies, and consequently, the number of capacitors on the DC-link as well. The topology, as shown in Fig. 1, allows obtaining three distinct output voltage levels. In this configuration, in all operating states for the three levels, two consecutive semiconductors are in continuous conduction, and the transition to half of the voltage on the DC-link is ensured through diodes D1 and D2. Table 1 contains the operating states for this configuration.

The current paths in the different operating states are illustrated in Fig. 2. The positive direction of the current is considered when it is in phase with the output voltage vfn, and the negative direction is considered when it is in opposition to vfn.

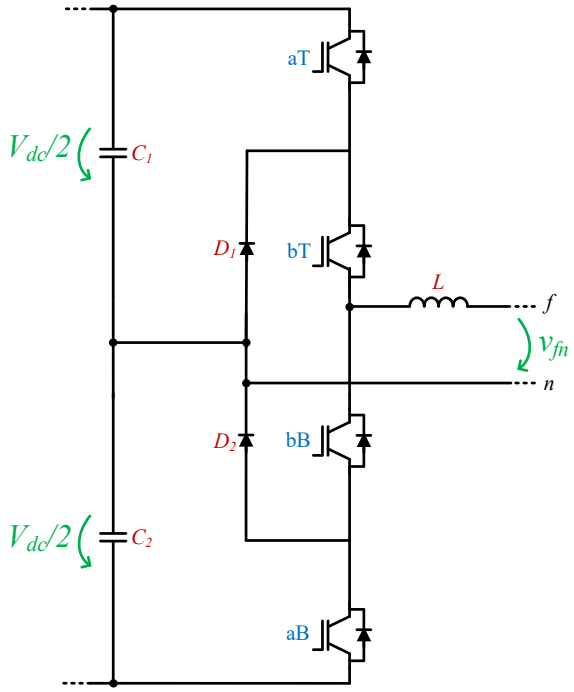

Figure 1. Schematic of the NPC (Neutral Point Clamped)
DC-AC Converter.

Table 1. Operating states of the NPC (Neutral Point Clamped) DC-AC Converter.

State	Switching Signals				Output Voltage (V)
	aT	*aB*	*bT*	*bB*	v_{fn}
1	1	1	0	0	$+V_{dC}/2$
2	0	1	1	0	0
3	0	0	1	1	$-V_{dC}/2$

Initially, in the state vfn = + Vdc/2, energy is transferred to the grid by the semiconductors aT and bT, and by the antiparallel diodes of both, in the situation where the energy flows from the load to the converter, as illustrated in Fig. 2 (b) and in Fig. 2 (a), respectively. In this converter, the transition to the negative level (-Vdc/2) requires passing through zero. This state is achieved by maintaining continuous conduction through semiconductors bT and bB. Both current directions in the state where zero is produced are shown in Fig. 2 (c) and Fig. 2 (d). In the last state, vfn = -Vdc/2, energy is transferred to the power grid using the semiconductors aB and bB, and by the antiparallel diodes of both, in the situation in which the energy is transferred to the converter, as shown in Fig. 2 (e) and Fig. 2 (f), respectively. The three-phase Neutral Point Clamped (NPC) DC-AC converter is composed of three single-phase topologies. In Fig. 3, the schematic of this converter is depicted.

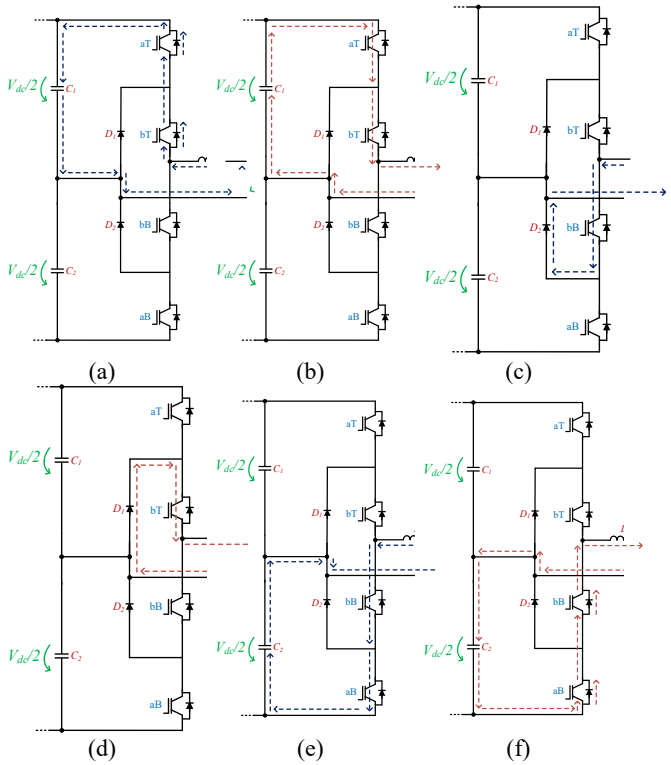

Figure 2. Operating states of the NPC DC-AC converter in the four quadrants: (a) Converter receiving energy with positive output voltage and negative current; (b) Converter supplying energy with positive output voltage and positive current; (c) Converter with zero output voltage and negative current; (d) Converter with zero output voltage and positive current; (e) Converter supplying energy with negative output voltage and negative current; (f) Converter receiving energy with negative output voltage and positive current.

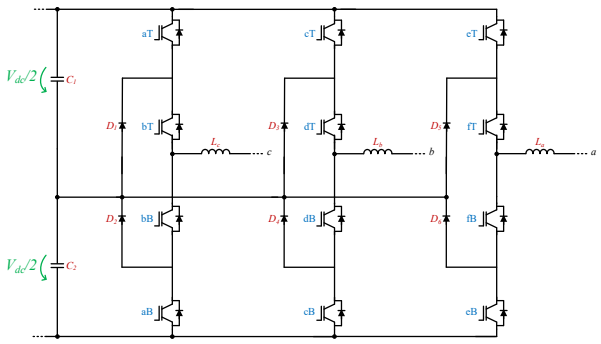

Figure 3. Schematic of the three-phase NPC DC-AC converter.

3. Control Algorithm of the Power Converter

This section presents the main distinct control algorithms of the power convert, including the specific algorithm for the modulation technique, the predictive current control, and the DC-link voltage control.

3.1. Modulation Technique

The increasing use of multi-level DC-AC converters is driven by the objective of enhancing the efficiency and performance of electrical systems. These converters offer improved output voltage quality through their stepped output voltage levels. However, the widespread adoption of these converters depends on the advancement of new modulation techniques capable of efficiently controlling more intricate converter configurations employing a larger number of power semiconductors. To achieve three or more levels, a higher number of carriers is typically employed, and there are various possible carrier configurations, with the main ones being level shifted or phase shifted [11]. The NPC topology readily accommodates a vertical phase shift between triangular waves, as each triangular wave can be associated with a pair of complementary IGBTs [12]. Level-shift carrier PWM requires a total of k-1 carriers, where k represents the number of levels in the DC-AC converter [9][13]. All carriers share the same frequency and amplitude, but each carrier has a distinct average value and is distributed vertically [10]. The vertical phase shift can be classified based on the arrangement of the carrier waves:

- Phase Disposition (PD): in this configuration, all carriers not only share the same frequency and amplitude but also align in phase. The only difference lies in the offset voltage, necessary to produce the vertical displacement.
- Phase Opposition Disposition (POD): in this arrangement, all carriers have the same frequency and amplitude, but they are in phase only within the same interval (positive or negative) due to a 180° phase shift between the positive and negative carriers.
- Alternative Phase Opposition Disposition (APOD): in this classification, the carriers are phase-shifted by 180° consecutively.

Fig. 4 illustrates each of the classifications described above, but it contains only two representations because there is no visible difference between POD and APOD for three levels.

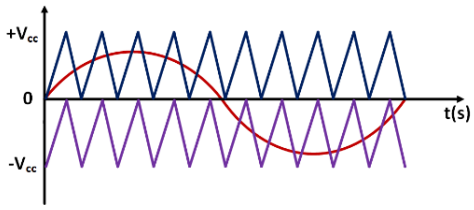

(a)

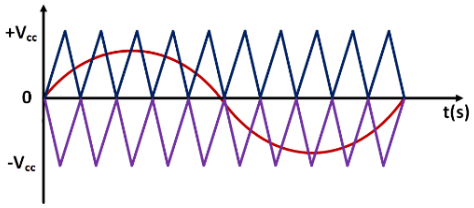

(b)

Figure 4. Multi-level SPWM modulation with vertical distribution: (a) Phase disposition; (b) Phase opposition disposition; (c) Alternative phase opposition disposition.

3.2. Grid-Side Current Control Technique

To achieve current control, the predictive current control technique has been chosen. This technique forecasts the required reference voltage (v*) to cancel the error between the output current and the reference current in the next sampling interval. The prediction is based on variations in the electrical system parameters, including the measured grid voltage and the inductance value of the coupling coil, along with other passive components (if used). This predictive approach is also known as Dead-beat control. The voltage-source DC-AC converter is connected to the electrical grid through a coupling coil. The grid voltage (vgrid) is equal to the voltage drop across the coupling coil (vL) plus the converter's output voltage (vout), as expressed in equation (1).

$$v_{grid} = v_L + v_{out} \tag{1}$$

Assuming the resistance value (RL) of the coupling coil is negligible, the following equation (2) is obtained, where iout represents the output current of the converter.

$$v_{grid} = L\frac{di_{out}}{dt} + v_{out} \tag{2}$$

The Euler method, shown in equation (3), can be employed to approximate the derivative component, considering a very small Δt (i.e., a high sampling frequency compared to the frequency of the synthesized signal). This results in a reliable prediction of the system's behavior.

$$\frac{di_{out}(t)}{dt} = \frac{i_{out}(t+\Delta t) - i_{out}(t)}{\Delta t} \tag{3}$$

By applying equation (3) to equation (2) and considering a sampling frequency $fa = 1/Ts$, we obtain the discrete-time equation (4).

$$v_{out}(k) = v_{grid}(k) - L\frac{i_{out}(k+1) - i_{out}(k)}{T_s} \tag{4}$$

Since this technique involves closed-loop control, the reference current at time [k+1] is equal to the current produced by the converter at time [k]. Thus, we can rewrite equation (4) as equation (5).

$$v_{out}(k) = v_{grid}(k) - L\frac{i^*(k) - i_{out}(k)}{T_s} \quad (5)$$

Hence, using equation (5), the reference voltage (vout = v*) for SPWM modulation is obtained. This technique is a linear control method that utilizes Sinusoidal Pulse Width Modulation (SPWM) to maintain a fixed switching frequency while delivering a rapid response to variations in the reference signal. However, this approach is sensitive to errors in system parameters or changes in them.

3.3. DC-Link Voltage Control Technique

Voltage control of the DC-link is achieved by using IGBT switching to adjust the DC-link voltage until it matches the reference voltage. This control is implemented in a multilevel AC-DC converter with a midpoint DC-link. To facilitate voltage regulation, two independent PI controllers are employed: one for controlling the voltage at the capacitor connected to the positive point of the DC-link (pdc1) and another for controlling the voltage at the capacitor connected to the negative point of the DC-link (pdc2). During the positive half-cycle of the grid voltage, the voltage control (vdc1) is executed, and during the negative half-cycle, the voltage control (vdc2) is applied. This ensures that both voltages are regulated consistently according to the reference voltage. To mitigate the influence of natural voltage DC-link oscillations inherent in the current control algorithm, a sliding window average of fa/fg samples is typically employed for vdc1 and vdc2, where fa is the sampling frequency and fg is the grid frequency. This approach helps to smooth out the voltage values, providing a more stable and consistent voltage regulation process. The stability and dynamic response of the DC-link control algorithm depend on the chosen parameters for the PI controller. Careful tuning of these parameters is crucial to achieve optimal performance and stability in the voltage regulation process.

4. Computational Validation

This chapter presents the computational simulations conducted in the PSIM software, essential for understanding and studying the topology. The simulation software PSIM, developed by Powersim Inc., offers numerous indispensable features for rigorous simulations, including a library with a wide range of components and the ability to create control system algorithms in the C language. Fig. 5 illustrates the simulation model implemented in the PSIM software.

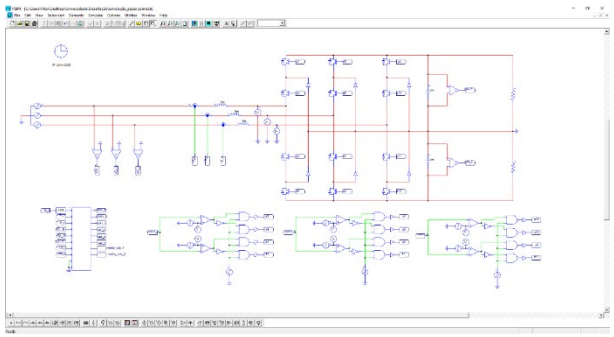

Figure 5. Simulation model of the system developed in PSIM, including the power converter and the digital control system.

Table 2. Relevant values used in computer simulation.

Parameter	Label	Value
Line-Line RMS Voltage	v_{ab}, v_{bc}, v_{ca}	400 V
DC-Link Voltage	v_{dc1}, v_{dc2}	400 V
DC-Link Capacitors	C_1, C_2	5 mF
Inductive Filters	L_a, L_b, L_c	5 mH
Switching Frequency	f_s	40 kHz
Sampling Frequency	f_a	40 kHz

In Table 2, some relevant values for components and ratings. Each DC-link voltage is 400 V, a necessary value for the interface with the electrical power grid of 230 V, 50 Hz. The power semiconductors switching frequency was arbitrated to 40 kHz. Regarding passive components, the inductive filters used were 5 mH, and the capacitors for the DC-link used were 5 mF. The modulation technique used was level-shift carrier PWM since each triangular wave can be associated with a pair of complementary IGBTs. Regarding the control of the system, results are presented using predictive current control and a PI controller to regulate DC-link voltage.

4.1. Grid-Side Current Control

With the objective to validate the predictive current control, a sinusoidal reference with approximately 15 A rms was used. Fig. 6 shows the currents generated by the converter acting as an active rectifier, and the electrical grid voltages, and it is evident that these currents are in phase with the electrical grid voltages.

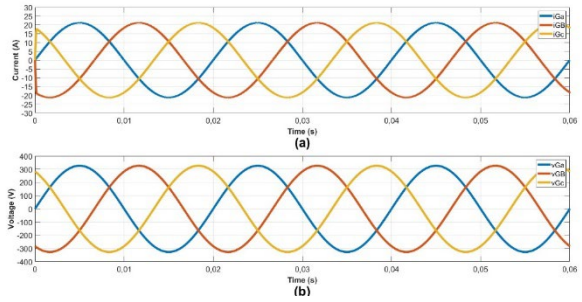

Figure 6. Results of the converter operating as an active rectifier: (a) Electrical grid currents; (b) Electrical grid voltages.

Regarding the current ripple generated by the converter, it is only 0.3 A, as shown in Fig. 7, which corresponds to 2% of the rms value of the generated current.

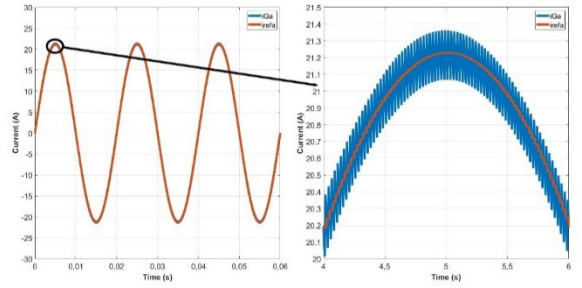

Figure 7. Results showing the detail of the current ripple in phase A, as well as the comparison between the current and its reference.

The modulation technique employed and detailed in section 3.1 was also rigorously validated through simulation. As depicted in Fig. 8, the converter generates three distinct levels per phase, while Fig. 9 illustrates the voltage across each conducting IGBT of phase A. For clarity, the representation includes only the IGBTs of phase A in the conducting state.

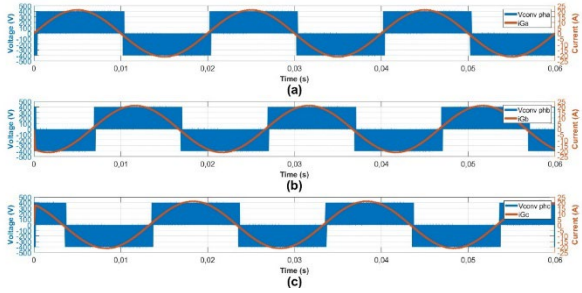

Figure 8. Results of the voltage levels generated by the converter per phase and current in each phase: (a) Phase A; (b) Phase B; (c) Phase C.

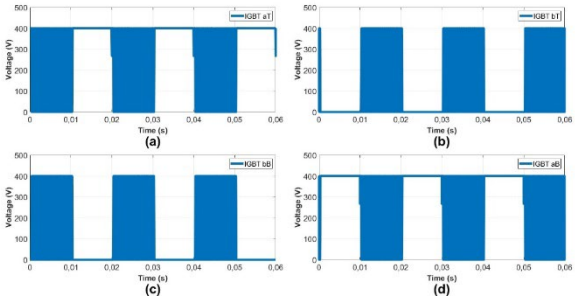

Figure 9. Results of the voltage across each IGBT of phase A: (a) IGBT aT; (b) IGBT bT; (c) IGBT bB; (d) IGBT aB.

To validate a sudden variation in the power absorbed by the load during the converter operation, the reference current was increased to nearly twice its previous value. As shown in the Fig. 10, it is evident that the currents generated by the converter also follow this increase.

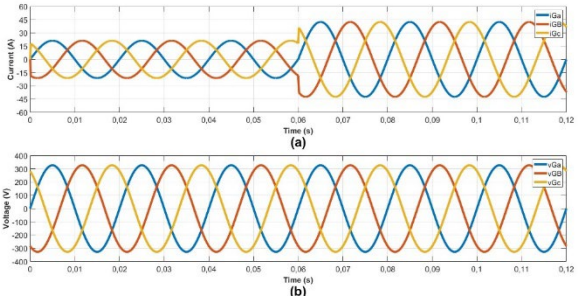

Figure 10. Results considering a sudden increase in power absorbed by the load: (a) Electrical grid currents; (b) Electrical grid voltages.

The converter's operation as an inverter was also validated with minor changes in the model. It simply required connecting DC voltage power supplies in parallel to the DC-link. In Fig. 11, it can be observed that the currents generated by the converter are in opposition to the electrical grid voltages.

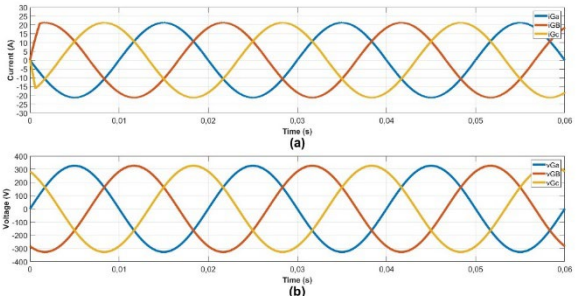

Figure 11. Results considering the converter operating as an inverter: (a) Electrical grid currents; (b) Electrical grid voltages.

Similarly to what was done in the rectifier operation mode, the converter was also validated as an inverter for a sudden variation in the power injected into the electrical grid, this time reduced to approximately half during the converter operation. As shown in Fig. 12, it is evident that the currents generated by the converter decrease and are in opposition to the electrical grid voltages.

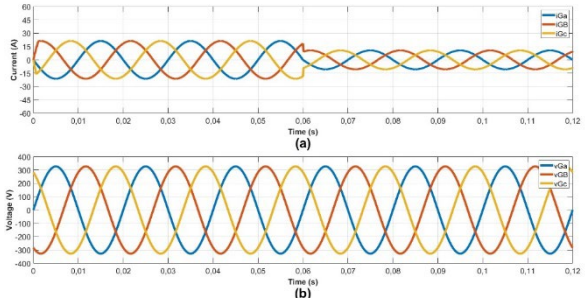

Figure 12. Results considering a sudden decrease in power injected into the electrical grid: (a) Electrical grid currents; (b) Electrical grid voltages.

4.2. DC-Link Voltage Control

To control the voltage of the DC-link , it was established that the resistive loads in the model shown in Fig. 5 would be 31 Ω each, resulting in an absorbed current of approximately 15 A rms per phase. To generate the reference current, the instantaneous value of the measured voltage at each DC-link was not used; instead, its average was obtained through the implementation of a digital sliding window average. Fig. 13 shows the steady-state results of the simple electrical grid voltages, current in each phase, and DC-link voltage, respectively.

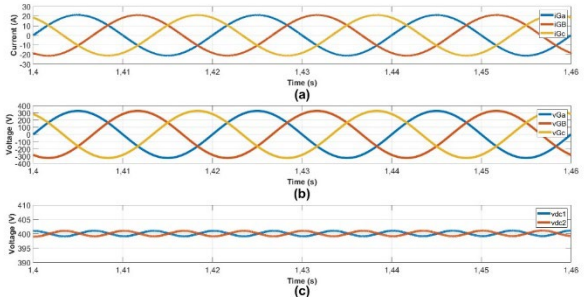

Figure 13. Results considering a steady-state operation with DC-Link voltage control: (a) Electrical grid currents; (b) Electrical grid voltages; (c) DC-link voltages.

As evident from Fig. 14 (c), the voltage ripple at each DC-link is approximately 2 V, representing about 0.5% of the steady-state value. Furthermore, during this operational mode, a sudden increase in power absorbed by the resistive loads was simulated by adding resistances in parallel, effectively doubling the power. The resulting grid currents and DC-link voltages are presented in Fig. 14.

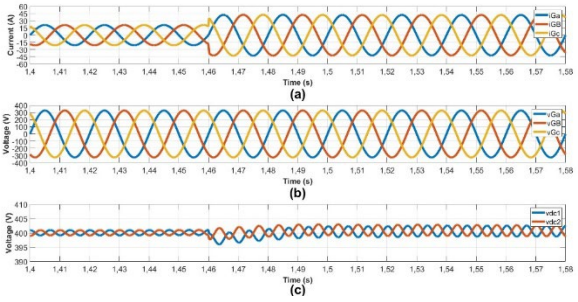

Figure 14. Results considering a sudden doubling of power absorbed by the load: (a) Electrical grid currents; (b) Electrical grid voltages; (c) DC-link voltages.

As observed in Fig. 14 (c), after five cycles of the grid, the voltages at both dc-links are balanced, with a slight increase in ripple to approximately 4 V. This represents around 1% of the steady-state value and a consequent doubling compared to the power absorbed prior to the variation.

5. Conclusions

This paper researches the importance of renewable energy sources and their application in the electrical power grid. The focus is on the implementation of a three-phase Neutral Point Clamped (NPC) DC-AC converter with a level-shift carrier PWM modulation technique and predictive current control. The use of multilevel converters, such as the NPC topology, offers several advantages over traditional two-level converters, including reduced harmonic distortion, lower dv/dt in power semiconductors, and increased efficiency. The level-shift carrier PWM modulation technique was employed to achieve three distinct output voltage levels, and predictive current control was chosen as the control algorithm due to its ability to rapidly respond to variations in the reference signal. Through computational simulations, using the PSIM software, the operation of the converter as active rectifier and inverter was successfully validated. The converter demonstrated the ability to adjust its current generation based on sudden variations in the power absorbed by the load and injected into the electrical grid. Additionally, the control of the DC-link voltage was effectively achieved, with a minimal voltage ripple of approximately 2 V, representing about 0.5% of the steady-state value. The findings from the simulations highlight the robustness and reliability of the proposed converter system, making it suitable for grid interconnection in renewable energy applications. By adopting renewable energy sources and advanced power electronics systems, societies can continue progressing towards a sustainable development,

reducing the environmental impact of electricity production, while improving energy efficiency and performance. It is hoped that the information presented in this paper will contribute to the advancement and adoption of renewable energy technologies for a greener and more sustainable future.

Acknowledgments

This work has been supported by FCT – Fundação para a Ciência e Tecnologia within the R&D Units Project Scope: UIDB/00319/2020.

References

[1] Maloberti, F., & Davies, A.C. (Eds.). (2016). A Short History of Circuits and Systems (1st ed.). River Publishers. https://doi.org/10.1201/9781003336938

[2] Patel, S., Larson, A., & Harvey, A. (2022, October 3). History of power: The evolution of the electric generation industry. POWER Magazine. https://www.powermag.com/history-of-power-the-evolution-of-the-electric-generation-industry/

[3] Sathaye, J., O. Lucon, A. Rahman, J. Christensen, F. Denton, J. Fujino, G. Heath, S. Kadner, M. Mirza, H. Rudnick, A. Schlaepfer, A. Shmakin, 2011: Renewable Energy in the Context of Sustainable Energy. In IPCC Special Report on Renewable Energy Sources and Climate Change Mitigation [O. Edenhofer, R. Pichs-Madruga, Y. Sokona, K. Seyboth, P. Matschoss, S. Kadner, T. Zwickel, P. Eickemeier, G. Hansen, S. Schlömer, C. von Stechow (eds)], Cambridge University Press, Cambridge, United Kingdom and New York, NY, USA.

[4] watchwire_admin. (2022, March 22). Distributed Energy Resources - the benefits of procuring them. WatchWire. https://watchwire.ai/distributed-energy-resources/

[5] Secretariat, R. (2022, June 15). Why is renewable energy important?. REN21. https://www.ren21.net/why-is-renewable-energy-important/

[6] eurostat. (2023, January 19). 22% of energy consumed in 2021 came from renewables. 22% of energy consumed in 2021 came from renewables - Products Eurostat News - Eurostat. https://ec.europa.eu/eurostat/en/web/products-eurostat-news/w/ddn-20230119-1

[7] Rauf, A.M.; Abdel-Monem, M.; Geury, T.; Hegazy, O. A Review on Multilevel Converters for Efficient Integration of Battery Systems in Stationary Applications. Energies 2023, 16, 4133. https://doi.org/ 10.3390/en16104133

[8] J. Rodriguez, J.-S. Lai, and F. Z. Peng, "Multilevel inverters: a survey of topologies, controls, and applications," IEEE Transactions on Industrial Electronics, Industrial Electronics, IEEE Transactions on, IEEE Trans. Ind. Electron., vol. 49, no. 4, pp. 724-724–738, 2002, doi: 10.1109/TIE.2002.801052.

[9] Barros, Luis A. M., António P. Martins, and José Gabriel Pinto. 2022. "A Comprehensive Review on Modular Multilevel Converters, Submodule Topologies, and Modulation Techniques" Energies 15, no. 3: 1078. https://doi.org/10.3390/en15031078

[10] V. Monteiro, J. G. Pinto, João C. Ferreira, Henrique Gonçalves, João L. Afonso "Bidirectional Multilevel Converter for Electric Vehicles," Annual Seminar on Automation, Industrial Electronics and Instrumentation 2012 - SAAEI'12, pp.434-439, Guimarães, Portugal, Jul. 2012, ISBN: 978-972-98603-5-5.

[11] S. Jawanjal, "Multilevel Inverter," International Research Journal of Engineering and Technology, 2017, [Online]. Available: www.irjet.net

[12] S. Kouro et al., "Recent advances and industrial applications of multilevel converters," IEEE Transactions on Industrial Electronics, vol. 57, no. 8, pp. 2553–2580, Aug. 2010, doi: 10.1109/TIE.2010.2049719.

[13] Vitor Monteiro, Nima Tashakor, Tiago Sousa, Tomas Kacetl, Stefan Götz, Joao L. Afonso, "Review of Five-Level Front-End Converters for Renewable-Energy Applications", Frontiers in Energy Research, 2020.